

The impact of AGN on the life of their host galaxies at $z \sim 2$

Chiara Circosta^{1,2}

¹European Southern Observatory, Karl-Schwarzschild-Str. 2,
85748 Garching bei München, Germany

²Dept. of Physics & Astronomy, University College London, Gower Street,
London WC1E 6BT, United Kingdom
email: c.circosta@ucl.ac.uk

Abstract. Feedback from active galactic nuclei (AGN) is thought to be key in shaping the life cycle of host galaxies by regulating star formation. Therefore, measuring the molecular gas reservoir out of which stars form is essential to understand the impact of AGN on star formation. In this talk I present an ongoing analysis to study the CO($J=3-2$) emission in a sample of 25 AGN at $z \sim 2$ using ALMA observations. The CO properties of our AGN have been compared to normal (non-AGN) star-forming galaxies. The comparison between the two samples reveals that, on average, the CO luminosities of AGN at high stellar masses ($\log(M_*/M_\odot) > 11$) are 0.5 dex lower than normal galaxies. We ascribe this difference to the AGN activity, which could be able to change the conditions of the gas through, e.g., excitation, heating or removal of CO.

Keywords. galaxies: active, galaxies: evolution, quasars: general, surveys, ISM: jets and outflows

1. Introduction

Active galactic nuclei (AGN) are powered by accreting supermassive black holes which release a huge amount of energy, injected into the surrounding interstellar medium (ISM). This energy, if efficiently coupled, could remove, heat and/or dissociate the molecular gas, that represents the fuel out of which stars form. The mechanisms by which the energy produced by the AGN is coupled to the ISM is called AGN feedback (Fabian 2012; King & Pounds 2015; Harrison 2017) and is thought to regulate the growth of the host galaxy. Despite being a necessary ingredient in models of galaxy evolution, proving the role of AGN feedback observationally remains a challenge.

A promising approach to move forward requires direct observations of the cold gas reservoir of galaxies through, for example, carbon monoxide (CO) rotational emission lines. The molecular gas provides an instantaneous measure of the raw fuel to form stars and a more direct tracer of potential feedback effects since it is less affected by the timescale issue, unlike the star formation rate (SFR). In particular, characterizing the cold gas phase of AGN host galaxies is key to understand whether this is different from inactive galaxies and quantify effects of AGN feedback on the host galaxy ISM.

Studies of local sources currently report no clear evidence for AGN to affect the ISM component of the host, by tracing the molecular phase (Husemann *et al.* 2017; Saintonge *et al.* 2017; Rosario *et al.* 2018), the atomic one (Ellison *et al.* 2019), and the dust mass as a proxy of the gas mass (Shangguan & Ho 2019). Interestingly, studies at redshift $z > 1$, near the peak of AGN and star-formation activity in the Universe ($z = 1 - 3$), present contrasting results. Reduced molecular gas fractions ($f_{gas} = M_{mol}/M_*$) are found in AGN

compared to the parent population of normal galaxies (Carilli & Walter 2013; Fiore *et al.* 2017; Kakkad *et al.* 2017; Brusa *et al.* 2018; Perna *et al.* 2018). This has been interpreted as an evidence for highly efficient gas consumption possibly related to AGN feedback affecting the gas reservoir of the host galaxies.

Nevertheless, these studies are plagued by several assumptions and limitations. CO measurements at $z > 1$ are usually performed using high- J transitions, and correction factors need to be assumed to estimate the luminosity of the ground-state transition as well as the gas mass. When dealing with SFRs of AGN hosts, an additional complication is the difficulty to properly account for the AGN contribution to the far-infrared luminosity. Different methods to estimate the AGN contribution can lead to different results and place the AGN population on the same star-formation law of normal galaxies (Kirkpatrick *et al.* 2019). Finally, AGN samples at high redshift are usually small and likely biased toward brighter objects (e.g. Brusa *et al.* 2018) or are heterogeneous when assembled from literature data (e.g. Fiore *et al.* 2017; Perna *et al.* 2018; Kirkpatrick *et al.* 2019).

Prompted by the need for a systematic and uniform study of the molecular gas content of AGN at $z \sim 2$, we are conducting an ALMA survey of 25 AGN to infer whether their activity affects the ISM of the host galaxy. Here we present the results of an ongoing analysis exploiting the CO($J = 3-2$) emission line as a tracer, which is the lowest- J transition accessible with ALMA at $z \sim 2$.

2. Sample selection

The sample of 25 AGN was drawn from the *COSMOS-Legacy* survey (Civano *et al.* 2016; Marchesi *et al.* 2016) and the wide-area *XMM-Newton* XXL survey North (Menzel *et al.* 2016; Pierre *et al.* 2016), by selecting targets with an absorption-corrected X-ray luminosity $L_X \geq 10^{42}$ erg s $^{-1}$ and secure spectroscopic redshift in the range $z = 2.0 - 2.5$. We followed Circosta *et al.* (2018) to collect the multi-wavelength data spanning from the X-rays to the radio regime and derive the properties of the targets through X-ray spectral analysis and broad-band spectral energy distribution fitting (e.g., stellar mass, SFR, bolometric and X-ray luminosities, obscuring column densities).

We built a comparison sample of star-forming galaxies which do not host an AGN (normal galaxies) by selecting sources from the PHIBSS sample (Tacconi *et al.* 2018), matched in redshift, stellar mass, SFR and CO transition with our AGN sample. By requiring that also the comparison sample is observed in CO($J = 3-2$), we are free from assumptions on the excitation correction, which can be crucial when comparing CO luminosities and bias the results (Kirkpatrick *et al.* 2019). The final sample of normal galaxies used in this work is composed of 47 objects.

In Fig. 1 we show the distribution of our AGN in the SFR- M_* plane, as well as the control sample. Of our AGN (normal galaxies), 44% (60%) sit on the MS, 40% (27%) above and 16% (13%) at the lower boundary of the MS. The coverage in AGN bolometric luminosity is around two orders of magnitude.

3. ALMA data

The dataset is made of ALMA observations carried out in Band 3 during Cycle 4 and 5 (Project codes: 2016.1.00798.S and 2017.1.00893.S; PI: V. Mainieri). The requested angular resolution was 1'' in order to probe the total gas reservoir of our targets. ALMA visibilities were calibrated using the CASA software version 4.7.0 for Cycle 4 data and 5.1.1 for Cycle 5, as originally used for the reduction with the pipeline. The final datacubes were generated with the CASA task CLEAN in velocity mode using "natural" weighting, cellsize of 0.2'' and velocity bin width of 24 km/s. Final products, generated

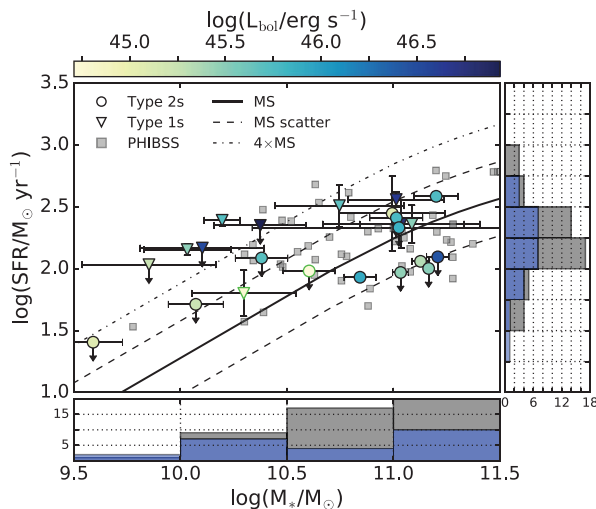


Figure 1. Distribution of host galaxy properties in the SFR- M_* plane for the 25 AGN (type 1s marked by triangles and type 2s marked by circles) in our sample and the comparison sample of normal galaxies (gray squares). The two data points with green edges represent the targets with SFR derived through modeling of the stellar emission with spectral energy distribution fitting. The color coding indicates the AGN bolometric luminosity for each object. The black solid line reproduces the main sequence of star-forming galaxies from Schreiber *et al.* (2015) at the average redshift of our target sample (i.e., ~ 2.3). The dashed lines mark the scatter of the main sequence (equal to 0.3 dex). The histograms show the projected distribution of the two quantities along each axis, in blue for our sample and gray for the comparison one.

from the continuum-subtracted uv datasets, have angular resolutions of 0.6–1.4". The sensitivity reached is 0.1–0.5 mJy per 100 km/s velocity bin.

Lines with $S/N \gtrsim 3$ are considered as detections. Moment 0 maps (i.e., the frequency-integrated flux maps) were constructed by using the task IMMOMENTS and collapsing along the channels with CO detection. The spectra were extracted from a region of the ALMA cubes with 2σ significance. We fit the line using a Gaussian model (Python package LMFIT) in order to retrieve widths and velocity-integrated fluxes. CO($J = 3-2$) is detected in 10 out of 25 targets. We measured FWHM in the range 80–700 km/s and CO($J = 3-2$) luminosities $\log(L'_{CO}/K \text{ km/s pc}^2) = 9.15-10.73$. For non detections, we derived the rms from the moment 0 maps by collapsing over a velocity width of 360 km/s (the average over the detections) and we then used 3σ upper limits for our analysis.

4. Comparison with normal galaxies

In Fig. 2 (*left*) we compare the distribution of L'_{CO} with the stellar masses of AGN and normal galaxies, color-coded by the offset in SFR with respect to the main sequence of star-forming galaxies. We use the CO($J = 3-2$) luminosity as a proxy of the molecular gas mass. To quantify the differences between the two samples, in Fig. 2 (*right*) we divided the targets in bins of stellar mass (width of 0.5 dex) and for each we computed the average L'_{CO} . In order to take into account upper limits, we performed a survival analysis by using the function KMESTM within the ASURV package, which gives the Kaplan-Meier estimator for the distribution function of a sample with upper limits. As for the comparison sample, the quantities shown in Fig. 2 (*right*) are the mean values for each stellar mass bin and the error bars represent the standard deviation of the distribution. The difference is not statistically significant in the lower mass bins ($\log(M_*/M_\odot) < 10.5$). However, there is a difference in L'_{CO} at the high mass end, which is particularly clear for

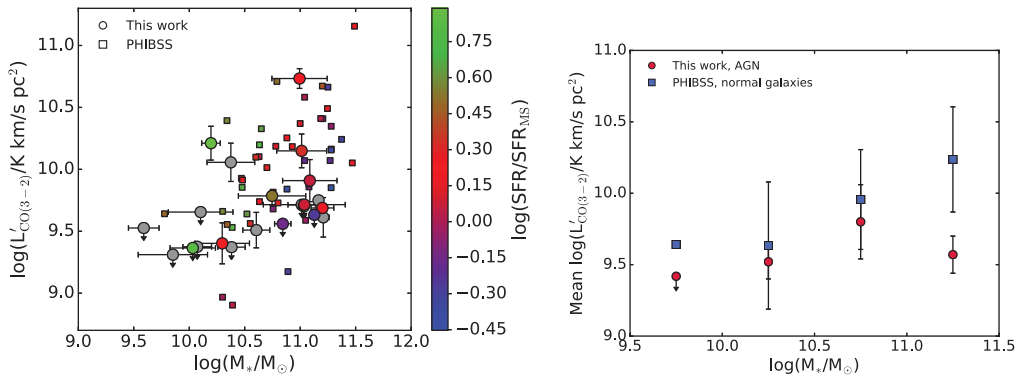


Figure 2. *Left:* L'_{CO} versus stellar masses for our sample of AGN (circles) and normal galaxies (squares; Tacconi *et al.* 2018). The color coding shows the deviation of the targets with respect to the MS (Schreiber *et al.* 2015). The targets with an upper limit in SFR are colored in gray. *Right:* mean L'_{CO} in bins of stellar mass (0.5 dex width) for AGN (circles) and normal galaxies (squares). Normal galaxies appear to have CO luminosities higher than AGN, with a difference of more than 0.5 dex in the high-mass bin.

$\log(M_*/M_\odot) > 11$. Normal galaxies appear to have CO luminosities higher than AGN, with a difference of more than 0.5 dex.

Previous work (Förster-Schreiber *et al.* 2019), studying outflows in galaxies through the H α emission line, found that incidence, strength, and velocity of AGN-driven winds is strongly correlated with stellar mass. In particular, high-velocity ($\sim 1000\text{--}2000 \text{ km s}^{-1}$) AGN-driven outflows are commonly detected at masses above $\log(M_*/M_\odot) = 10.7$. This is the same stellar-mass threshold above which the difference in CO luminosity between AGN and normal galaxies in our analysis is significant. A deficit of CO emission in the CO($J=3-2$) transition has been recently found by Kirkpatrick *et al.* (2019). They performed a study of CO transitions for a literature sample spanning from normal galaxies to powerful AGN and found lower CO($J=3-2$) and CO($J=1-0$) fluxes for AGN than normal galaxies. Such result is in agreement with what we found for our samples and would translate in lower gas masses in high-redshift AGN. Similarly, Fiore *et al.* (2017) compared molecular gas and stellar masses for an heterogeneous AGN sample collected from the literature and found lower gas masses in AGN than in normal galaxies.

The difference in CO luminosity between the population of AGN and normal galaxies could be ascribed to the presence of the AGN. The central engine may have a role in heating, exciting, dissociating and/or ejecting the gas. However, understanding the mechanism producing such difference requires further data and larger samples, tracing different gas phases and several CO transitions.

5. Interpretation of our results

Possible scenarios to interpret our results are as follows.

The gas is excited by the AGN to higher- J transitions. According to previous work (Weiß *et al.* 2007; Carilli & Walter 2013), the molecular gas of AGN could therefore be more excited than in normal galaxies and, as a consequence, we observe less CO emission in the lower- J transitions. At high redshift the sampling of CO transitions is usually sparser than in the Local Universe, but variations in the line fluxes connected with the presence of an AGN were reported (Carilli & Walter 2013; Brusa *et al.* 2018; Carniani *et al.* 2019). Studies of several CO transitions over large AGN samples, especially out to high- J , are needed to understand the role of AGN ionization in shaping the properties of the molecular gas reservoir.

The gas is heated/dissociated by the AGN. An interesting example of this scenario was recently presented by Rosario *et al.* (2019). Spatially-resolved observations of different gas phases (both molecular and ionized) for a nearby Seyfert 2 galaxy revealed a central region (< 200 pc) which is weak in CO($J=2-1$) emission but filled with ionized and warm molecular gas (H_2 MIR rotational lines). The energy liberated by the AGN may influence the molecular gas properties and suppress the CO($J=2-1$) emission by heating and dissociating the molecular gas. At high redshift, when the overall AGN population is more active, the central engine could have an impact over larger spatial scales.

AGN-driven outflows affect the gas reservoir. Another possible effect of the AGN activity on the molecular gas is through outflows. This possibility is supported by observations of individual objects. For example, Brusa *et al.* (2018) found low gas fraction in a powerful AGN at $z \sim 1.6$ hosting also a high-velocity molecular and ionized outflow. AGN feedback in action in this target could be depleting the molecular gas reservoir. As for our sample, we are performing a systematic investigation of the ionized gas phase with SINFONI at the ESO's Very Large Telescope as part of the SINFONI Survey for Unveiling the Physics and Effect of Radiative feedback (SUPER; Circosta *et al.* 2018). These data, available for 19 out of 25 targets, will reveal the presence of outflows.

References

- Brusa, M., Cresci, G., Daddi, E., *et al.* 2018, *A&A*, 612, 29
 Carilli, C. L. & Walter, F. 2013, *ARAA*, 51, 105
 Carniani, S., Gallerani, S., Vallini, L., *et al.* 2019, *MNRAS*, 489, 3939
 Circosta, C., Mainieri, V., Padovani, P., *et al.* 2018, *A&A*, 620, 82
 Civano, F., Marchesi, S., Comastri, A., *et al.* 2016, *ApJ*, 819, 62
 Ellison, S. L., Brown, T., Catinella, B., & Cortese, L. 2019, *MNRAS*, 482, 5694
 Fabian, A. C. 2012, *ARAA*, 50, 455
 Fiore, F., Feruglio, C., Shankar, F., *et al.* 2017, *A&A*, 601, 143
 Förster Schreiber, N. M., Übler, H., Davies, R. L., *et al.* 2019, *ApJ*, 875, 21
 Harrison, C. M. 2017, *Nature Astronomy*, 1, 165
 Husemann, B., Davis, T. A., Jahnke, K., *et al.* 2017, *MNRAS*, 470, 1570
 Kakkad, D., Mainieri, V., Brusa, M., *et al.* 2017, *MNRAS*, 468, 4205
 King, A. & Pounds, K. 2015, *ARAA*, 53, 115
 Kirkpatrick, A., Sharon, C., Keller, Pope, A., *et al.* 2019, *ApJ*, 879, 41
 Marchesi, S., Civano, F., Elvis, M., *et al.* 2016, *ApJ*, 817, 34
 Menzel, M.-L., Merloni, A., Georgakakis, A., *et al.* 2016, *MNRAS*, 457, 110
 Noeske, K. G., Weiner, B. J., Faber, S. M., *et al.* 2007, *ApJL*, 660, 43
 Perna, M., Sargent, M. T., Brusa, M., *et al.* 2018, *A&A*, 619, 90
 Pierre, M., Pacaud, F., Adami, C., *et al.* 2016, *A&A*, 592, 1
 Rosario, D. J., Burtscher, L., Davies, R. I., *et al.* 2018, *MNRAS*, 473, 5658
 Rosario, D. J., Togi, A., Burtscher, L., *et al.* 2019, *ApJ*, 875, 8
 Saintonge, A., Catinella, B., Tacconi, L. J., *et al.* 2017, *ApJS*, 233, 22
 Schreiber, C., Pannella, M., Elbaz, D., *et al.* 2015, *A&A*, 575, 74
 Shanguan, J. & Ho, L. C. 2019, *ApJ*, 873, 90
 Tacconi, L. J., Genzel, R., Saintonge, A., *et al.* 2018, *ApJ*, 853, 179
 Weiß, A., Downes, D., Neri, R., *et al.* 2007, *A&A*, 467, 955